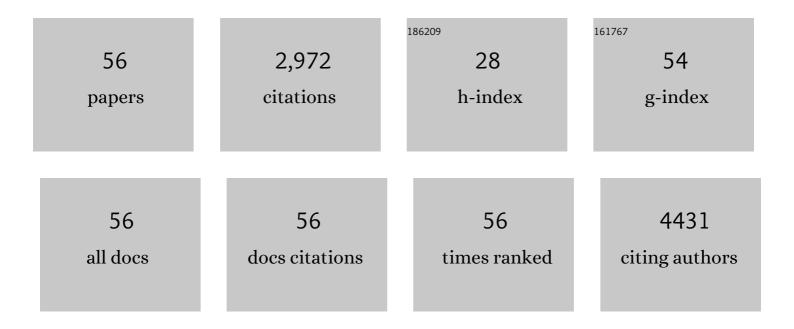
Tao Ding

List of Publications by Year in descending order

Source: https://exaly.com/author-pdf/1932451/publications.pdf Version: 2024-02-01



#	Article	IF	CITATIONS
1	Laser-assisted high-performance PtRu alloy for pH-universal hydrogen evolution. Energy and Environmental Science, 2022, 15, 102-108.	15.6	66
2	NiTe ₂ Nanosheets for Broadband Photodetection. ACS Applied Nano Materials, 2022, 5, 6094-6099.	2.4	6
3	Electron and Hole Spin Relaxation in CdSe Colloidal Nanoplatelets. Journal of Physical Chemistry Letters, 2021, 12, 86-93.	2.1	13
4	Synergistic Modulation at Atomically Dispersed Fe/Au Interface for Selective CO ₂ Electroreduction. Nano Letters, 2021, 21, 686-692.	4.5	41
5	A superficial sulfur interfacial control strategy for the fabrication of a sulfur/carbon composite for potassium–sulfur batteries. Chemical Communications, 2021, 57, 1490-1493.	2.2	19
6	Spin blockade and phonon bottleneck for hot electron relaxation observed in n-doped colloidal quantum dots. Nature Communications, 2021, 12, 550.	5.8	23
7	In Situ Investigation on Doping Effect in Co-Doped Tungsten Diselenide Nanosheets for Hydrogen Evolution Reaction. Journal of Physical Chemistry C, 2021, 125, 6229-6236.	1.5	16
8	Atomically Precise Dinuclear Site Active toward Electrocatalytic CO ₂ Reduction. Journal of the American Chemical Society, 2021, 143, 11317-11324.	6.6	153
9	Regulating the Coordination Environment of Ruthenium Cluster Catalysts for the Alkaline Hydrogen Evolution Reaction. Journal of Physical Chemistry Letters, 2021, 12, 8016-8023.	2.1	21
10	Insight into Fe Activating One-Dimensional α-Ni(OH) ₂ Nanobelts for Efficient Oxygen Evolution Reaction. Journal of Physical Chemistry C, 2021, 125, 20301-20308.	1.5	17
11	Plasmon-assisted photocatalytic CO ₂ reduction on Au decorated ZrO ₂ catalysts. Dalton Transactions, 2021, 50, 6076-6082.	1.6	16
12	Marcus inverted region of charge transfer from low-dimensional semiconductor materials. Nature Communications, 2021, 12, 6333.	5.8	27
13	Mechanisms of triplet energy transfer across the inorganic nanocrystal/organic molecule interface. Nature Communications, 2020, 11, 28.	5.8	127
14	Tuning Intermediate-Band Cu ₃ VS ₄ Nanocrystals from Plasmonic-like to Excitonic via Shell-Coating. Chemistry of Materials, 2020, 32, 224-233.	3.2	13
15	Synthesis and Spectroscopy of Monodispersed, Quantum-Confined FAPbBr ₃ Perovskite Nanocrystals. Chemistry of Materials, 2020, 32, 549-556.	3.2	39
16	Dynamic Surface Reconstruction of Single-Atom Bimetallic Alloy under <i>Operando</i> Electrochemical Conditions. Nano Letters, 2020, 20, 8319-8325.	4.5	28
17	Coulomb Barrier for Sequential Two-Electron Transfer in a Nanoengineered Photocatalyst. Journal of the American Chemical Society, 2020, 142, 13934-13940.	6.6	19
18	<i>Operando</i> evidence of Cu ⁺ stabilization <i>via</i> a single-atom modifier for CO ₂ electroreduction. Journal of Materials Chemistry A, 2020, 8, 25970-25977.	5.2	26

ΤΑΟ DING

#	Article	IF	CITATIONS
19	Triplet Energy Transfer from Perovskite Nanocrystals Mediated by Electron Transfer. Journal of the American Chemical Society, 2020, 142, 11270-11278.	6.6	82
20	Size―and Halideâ€Dependent Auger Recombination in Lead Halide Perovskite Nanocrystals. Angewandte Chemie - International Edition, 2020, 59, 14292-14295.	7.2	63
21	Size―and Halideâ€Dependent Auger Recombination in Lead Halide Perovskite Nanocrystals. Angewandte Chemie, 2020, 132, 14398-14401.	1.6	8
22	Molybdenum disulfide with enlarged interlayer spacing decorated on reduced graphene oxide for efficient electrocatalytic hydrogen evolution. Journal of Materials Science, 2020, 55, 6637-6647.	1.7	59
23	Spin-Controlled Charge-Recombination Pathways across the Inorganic/Organic Interface. Journal of the American Chemical Society, 2020, 142, 4723-4731.	6.6	25
24	Observation of a phonon bottleneck in copper-doped colloidal quantum dots. Nature Communications, 2019, 10, 4532.	5.8	52
25	On the absence of a phonon bottleneck in strongly confined CsPbBr ₃ perovskite nanocrystals. Chemical Science, 2019, 10, 5983-5989.	3.7	71
26	Triplet Energy Transfer from CsPbBr ₃ Nanocrystals Enabled by Quantum Confinement. Journal of the American Chemical Society, 2019, 141, 4186-4190.	6.6	169
27	Quantum-Cutting Luminescent Solar Concentrators Using Ytterbium-Doped Perovskite Nanocrystals. Nano Letters, 2019, 19, 338-341.	4.5	153
28	Biexciton Auger recombination in mono-dispersed, quantum-confined CsPbBr3 perovskite nanocrystals obeys universal volume-scaling. Nano Research, 2019, 12, 619-623.	5.8	63
29	In Situ Construction of Small Pt NPs Embedded in 3D Spherical Porous Carbon as an Electrocatalyst for Liquid Fuel Oxidation with High Performance. ACS Omega, 2018, 3, 17668-17675.	1.6	1
30	Lighting Up AlEgen Emission in Solution by Grafting onto Colloidal Nanocrystal Surfaces. Journal of Physical Chemistry Letters, 2018, 9, 6334-6338.	2.1	5
31	"Intact―Carrier Doping by Pump–Pump–Probe Spectroscopy in Combination with Interfacial Charge Transfer: A Case Study of CsPbBr ₃ Nanocrystals. Journal of Physical Chemistry Letters, 2018, 9, 3372-3377.	2.1	42
32	Electron Transfer into Electron-Accumulated Nanocrystals: Mimicking Intermediate Events in Multielectron Photocatalysis II. Journal of the American Chemical Society, 2018, 140, 10117-10120.	6.6	20
33	Carrier-doping as a tool to probe the electronic structure and multi-carrier recombination dynamics in heterostructured colloidal nanocrystals. Chemical Science, 2018, 9, 7253-7260.	3.7	6
34	Component‶unable Rutileâ€Anatase TiO ₂ /Reduced Graphene Oxide Nanocomposites for Enhancement of Electrocatalytic Oxygen Evolution. ChemNanoMat, 2018, 4, 1133-1139.	1.5	13
35	Charge Transfer from n-Doped Nanocrystals: Mimicking Intermediate Events in Multielectron Photocatalysis. Journal of the American Chemical Society, 2018, 140, 7791-7794.	6.6	37
36	Monodisperse Ternary NiCoP Nanostructures as a Bifunctional Electrocatalyst for Both Hydrogen and Oxygen Evolution Reactions with Excellent Performance. Advanced Materials Interfaces, 2016, 3, 1500454.	1.9	132

ΤΑΟ DING

#	Article	IF	CITATIONS
37	A highly active and durable CuPdPt/C electrocatalyst for an efficient hydrogen evolution reaction. Journal of Materials Chemistry A, 2016, 4, 15309-15315.	5.2	29
38	Fabrication of amorphous CoMoS ₄ as a bifunctional electrocatalyst for water splitting under strong alkaline conditions. Nanoscale, 2016, 8, 18887-18892.	2.8	91
39	Self-assembly growth of alloyed NiPt nanocrystals with holothuria-like shape for oxygen evolution reaction with enhanced catalytic activity. APL Materials, 2016, 4, .	2.2	2
40	Design and Epitaxial Growth of MoSe ₂ –NiSe Vertical Heteronanostructures with Electronic Modulation for Enhanced Hydrogen Evolution Reaction. Chemistry of Materials, 2016, 28, 1838-1846.	3.2	310
41	Controlled Synthesis of Ultrathin Sb ₂ Se ₃ Nanowires and Application for Flexible Photodetectors. Advanced Science, 2015, 2, 1500109.	5.6	84
42	Alternative Synthesis of CuFeSe ₂ Nanocrystals with Magnetic and Photoelectric Properties. ACS Applied Materials & Interfaces, 2015, 7, 2235-2241.	4.0	54
43	Fabrication of Ultrathin Bi ₂ S ₃ Nanosheets for Highâ€Performance, Flexible, Visible–NIR Photodetectors. Small, 2015, 11, 2848-2855.	5.2	205
44	Synthesis of Cu ₂ SnSe ₃ –Au heteronanostructures with optoelectronic and photocatalytic properties. Nanoscale, 2015, 7, 15106-15110.	2.8	27
45	Phosphine-Free Synthesis and Characterization of Cubic-Phase Cu2SnTe3 Nanocrystals with Optical and Optoelectronic Properties. Chemistry of Materials, 2015, 27, 6181-6184.	3.2	27
46	3D architecture constructed via the confined growth of MoS ₂ nanosheets in nanoporous carbon derived from metal–organic frameworks for efficient hydrogen production. Nanoscale, 2015, 7, 18004-18009.	2.8	82
47	Modifying the symmetry of colloidal photonic crystals: a way towards complete photonic bandgap. Journal of Materials Chemistry C, 2014, 2, 4100.	2.7	16
48	Fast colloidal synthesis of scalable Mo-rich hierarchical ultrathin MoSe _{2â^'x} nanosheets for high-performance hydrogen evolution. Nanoscale, 2014, 6, 11046-11051.	2.8	200
49	Organometallic-Route Synthesis, Controllable Growth, Mechanism Investigation, and Surface Feature of PbSe Nanostructures with Tunable Shapes. Langmuir, 2014, 30, 2863-2872.	1.6	16
50	Epitaxial growth of bulky calcite inverse opal induced by a single crystalline calcite substrate. CrystEngComm, 2014, 16, 7617.	1.3	1
51	Anisotropic oxygen plasma etching of colloidal particles in electrospun fibers. Chemical Communications, 2011, 47, 2429-2431.	2.2	16
52	Patterning and pixelation of colloidal photonic crystals for addressable integrated photonics. Journal of Materials Chemistry, 2011, 21, 11330.	6.7	31
53	Oxygen Plasma Etching-Induced Crystalline Lattice Transformation of Colloidal Photonic Crystals. Journal of the American Chemical Society, 2010, 132, 17340-17342.	6.6	23
54	Controlled Directionality of Ellipsoids in Monolayer and Multilayer Colloidal Crystals. Langmuir, 2010, 26, 11544-11549.	1.6	30

#	Article	IF	CITATIONS
55	Bottom-Up Photonic Crystal Approach with Top-Down Defect and Heterostructure Fine-Tuning. Langmuir, 2010, 26, 4535-4539.	1.6	23
56	Photonic Crystals of Oblate Spheroids by Blown Film Extrusion of Prefabricated Colloidal Crystals. Langmuir, 2009, 25, 10218-10222.	1.6	34